Connection between nuclear structure, dissipation, and time in fission data

Connection between nuclear structure, dissipation, and time in fission data

M. Caamaño[1,*], D. Ramos[2], D. Fernández[1], G. Mantovani[3,4,1], F. Farget[2], C. Rodríguez-Tajes[2], A. Lemasson[2], M. Rejmund[2], C. Schmitt[5], D. Ackermann[2], H. Álvarez-Pol[1], L. Audouin[6], J. Benlliure[1], S. Biswas[2], E. Casarejos[7], E. Clement[2], D. Cortina[1], O. Delaune[2], X. Derkx[2], A. Dijon[2], D. Doré[8], D. Durand[9], J. D. Frankland[2], B. Fernández-Domínguez[1], G. de France[2], M. O. Fregeau[2], D. Galaviz[10], E. Galiana-Baldó[1], A. Heinz[11], A. Henriques[10], B. Jacquot[2], B. Jurado[12], Y. H. Kim[2], P. Morfouace[2], C. Paradela[1], J. Piot[2], D. Ralet[13], T. Roger[2], M. D. Salsac[8], P. Teubig[10], and I. Tsekhanovich[12]

[1]IGFAE - Universidade de Santiago de compostela, E-15706 Santiago de Compostela, Spain
[2]GANIL, CEA/DSM–CNRS/IN2P3, BP 55027, F–14076 Caen Cedex 5, France
[3]INFN, Laboratori Nazionali di Legnaro, Legnaro (Padova), Italy
[4]Universitá degli Studi di Padova, Padova, Italy
[5]IPHC Strasbourg, Université de Strasbourg-CNRS/IN2P3, Strasbourg Cedex, France
[6]IJC Lab, Université Paris-Saclay, CNRS/IN2P3, Orsay, France
[7]Universidade de Vigo, E-36310 Vigo, Spain
[8]CEA Saclay, DRF/IRFU/SPhN, 91191 Gif-sur-Yvette Cedex, France
[9]LPC Caen, Université de Caen Basse-Normandie, ENSICAEN-CNRS/IN2P3, Caen Cedex, France
[10]Universidade de Lisboa, Lisbon, Portugal
[11]Chalmers University of Technology, Göteborg, Sweden
[12]CENBG, IN2P3/CNRS-Université de Bordeaux, Gradignan Cedex, France
[13]CSNSM, CNRS/IN2P3, Université de Paris-Saclay, Orsay, France

Abstract. Nuclear fission is still one of the most complex physical processes due to the interplay between macroscopic and microscopic nuclear properties that decide the output. An example of this coupling is the presence of nuclear dissipation as an important ingredient that contributes to drive the dynamics and has a clear impact on the time of the process. However, different theoretical interpretations and scarce experimental data make it poorly understood. At low excitation energy, the relative yields of fragments even and odd atomic numbers show a clear difference, which can be quantified with the so-called even-odd effect. This seemingly mundane property can be used to obtain information about the energy dissipated during the process and the role of structure in its dynamics.
In this paper, the study of the even-odd effect for elastic- and transfer-induced fission data is discussed. A clear connection with particular fragment shells and the dissipation energy is found, as detailed in Ref. [1]. In addition, preliminary results from quasi-fission data show the formation of a relatively large even-odd effect, which suggests a process with low dissipation mainly consisting in the exchange of nucleon pairs.

1 Introduction

One of the challenges that the study of nuclear fission still faces is the complete determination of the energy balance between the fragments and the different components. The mass of the fissioning system and the initial excitation energy is transformed into the final kinetic and excitation energies of the fragments. The excitation energy is released in neutron and γ emission as the fragments evolve towards their ground states, which makes it a potential experimental observable. However, relevant information on the process between the saddle and scission points is contained and mixed within the fragments excitation energy: the total excitation energy (TXE) is the sum of the energy used in collective degrees of freedom as the deformation of the fragments ($E^{*,\mathrm{def}}$) and the excitation of normal modes ($E^{*,\mathrm{col}}$), and the intrinsic excitation energy ($E^{*,\mathrm{int}}$), stored in the form of single-particle excitations. And, within $E^{*,\mathrm{int}}$, the energy dissipated between saddle and scission ($E^{*,\mathrm{dis}}$) is added to the initial excitation energy above the barrier ($E^{*,\mathrm{Bf}}$). Figure 1 shows a simplified graphical representation of these components.

The actual distribution of these energy components reflects properties of the fission process. For instance, the sum of TXE and $E^{*,\mathrm{def}}$ would give a still image of the potential landscape at the scission stage, while $E^{*,\mathrm{dis}}$ is closely link to the diabatic character of the process and to the time of the evolution from the saddle configuration to the moment of scission [2–7], although the specific role and impact are still to be fully understood.

In this paper, a method to obtain the dissipation energy $E^{*,\mathrm{dis}}$ from the even-odd staggering in isotopic fragment yields is presented. The results show a clear dependence of

*e-mail: manuel.fresco@usc.es

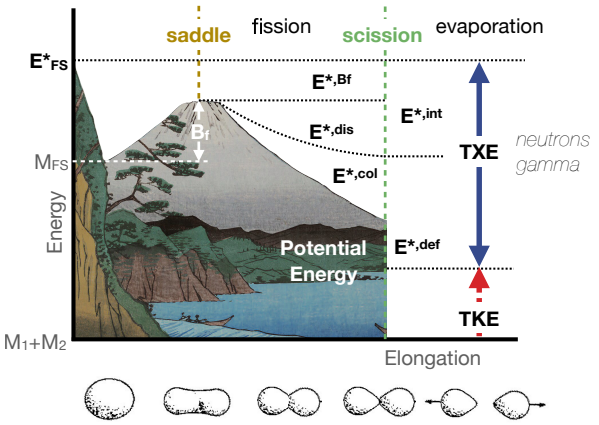

Figure 1. Schematic description of the energy components of the fission process. A fissioning system with a mass $M_{\rm FS}$ and an initial excitation energy $E^*_{\rm FS}$ elongates towards the saddle point overcoming a fission barrier with a $B_{\rm f}$. In its descent to the scission point, the difference in potential energy is converted in collective normal modes $E^{*,\rm col}$ and dissipation energy $E^{*,\rm dis}$, which is added to the excitation energy above the barrier $E^{*,\rm Bf}$. Once the fragments split at the scission point, they fly apart with a total kinetic energy TKE, while the intrinsic excitation energy $E^{*,\rm int}$, and the collective and deformation energy $E^{*,\rm def}$ gained in the process form the total excitation energy TXE of the fragments, which is released as neutron and γ evaporation. Other components, like pre-scission kinetic energy, are not displayed for simplicity.

$E^{*,\rm dis}$ with particular proton numbers, which suggests different fission times for different fragment configurations. A detailed discussion of this study can be found in [1]. In addition, a preliminary study of the even-odd staggering and its relation with dissipation in quasi-fission reactions is discussed.

2 Proton even-odd staggering, intrinsic excitations, and proton shells

As soon as experimental data on isotopic fragment yields were available (i.e. the production of fragments according their atomic number Z) it was readily evident that even-Z fragments were more produced than odd-Z ones [8]. Indeed, the observation of odd-Z fragments produced from low-energy, even-Z fissioning systems indicates that proton pairs are broken along the fission process and is also a proof of a form of dissipation in the path from saddle to scission.

The amplitude of this even-odd staggering in the isotopic yields can be evaluated as the normalised difference between even- and odd-Z yields: $\delta = (\sum Y_{\rm even} - \sum Y_{\rm odd})/\sum Y$. Measurements of δ as a function of the initial $E^*_{\rm FS}$ revealed a close connection between the even-odd effect and intrinsic excitation energy [9, 10], suggesting that δ can be used as an observable for the amount of $E^{*,\rm int}$ produced in the process, allowing a separation between collective and intrinsic components in TXE. In particular, the relation between δ and $E^{*,\rm Bf}$ includes the pairing gap Δ and an offset δ_0: $E^{*,\rm Bf} - \Delta \approx -G[\ln(\delta) - \ln(\delta_0)]$.

Upon close inspection, it is not difficult to realise that the amplitude of the even-odd staggering is not constant for all fragment splits. In order to explore this dependence, it is not unusual to use formulas to deduce the local even-odd effect δ_Z, which give an average value of the even-odd effect in a reduced region of fragment Z. One of the most widely used formulas was proposed in Ref. [11], which estimates an average δ_Z in four consecutive Z assuming an underlying Gaussian distribution.

The study of δ_Z has revealed the role of level density in the rearrangement of single protons among the pre-fragments, which, in turn, drive the resulting δ_Z. In short, single protons are drawn to higher level densities, which results in an increase of δ_Z as a function of the asymmetry of the split, and in the fact that odd-Z fissioning systems display a negative δ_Z in the heavy fragment side [12]. This mechanism adds to the underlying probability of pair breaking that depends on the available energy [13, 14].

2.1 Experimental data from VAMOS

For a number of years already, the large-acceptance VAMOS spectrometer at GANIL (France) hosts a research line on fission [1, 15–23]. So far, actinides and sub-lead fissioning systems were studied at low and high excitation energies with inelastic-, transfer- and fusion-induced reactions. The advantages of this setup include a precise determination of the initial $E^*_{\rm FS}$, a complete fragment identification in mass and atomic numbers, and the measurement of their velocity vectors in the c.m. of the fissioning system.

In one of these experiments, δ_Z was measured for a set of fissioning systems at different $E^{*,\rm Bf}$. Figure 2 shows the collection of $\delta_Z(Z, E^{*,\rm Bf})$ for ^{238}U, ^{239}Np, and ^{240}Pu (data from [1, 24, 25]). Some observations can be drawn from these measurements: a) an increase of $|\delta_Z|$ with the asymmetry of the split appears for all systems and all $E^{*,\rm Bf}$; b) the odd-Z system ^{239}Np displays a negative δ_Z in the heavy fragment; and c) there is a clear positive δ_Z peak around Z=50 for all systems, including ^{239}Np.

While the first two observations are expected from previous measurements, the existence of a positive peak at Z=50 reveals a new feature around the spherical shell at the barrier: irrespective of the even- or odd-Z character of the fissioning system, Z=50 is preferably formed completely paired and, only after, the level density modifies the strength of the peak in the descent towards the scission point.

This section summarises some of the methods and conclusions of Ref. [1], where further details can be found.

2.2 Dissipation energy from even-odd effect measurements

Assuming that the dissipation energy $E^{*,\rm dis}$ has a weak dependence on the initial $E^*_{\rm FS}$, the relation between δ_Z and $E^{*,\rm Bf}$ can be rewritten as

$$E^{*,\rm dis}(Z) + [E^{*,\rm Bf} - \Delta] = G(Z)\ln(|\delta_Z|), \qquad (1)$$

when $E^{*,\rm Bf} > \Delta$. For $E^{*,\rm Bf} < \Delta$, δ_Z is observed to remain constant [9, 10, 13].

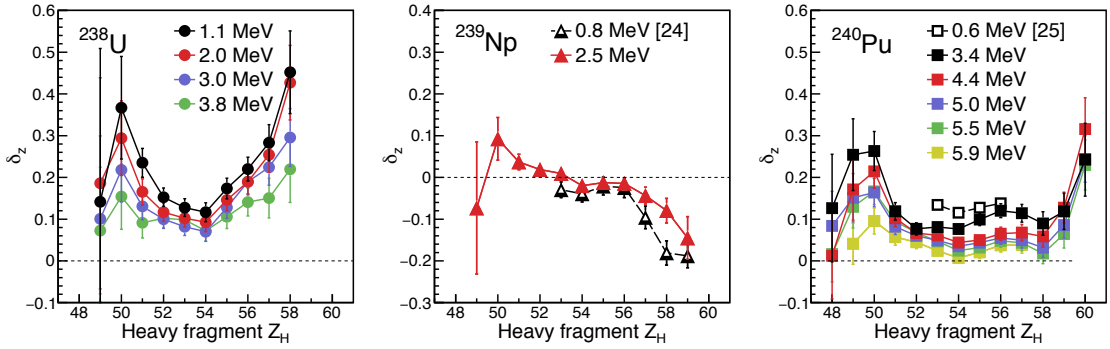

Figure 2. Local even-odd effect δ_Z as a function of the heavy-fragment Z for ^{238}U (left), ^{239}Np (middle) with data from [24] (dashed line with empty symbols), and ^{240}Pu (right) with data from [25] (dashed line with empty symbols). Each line and color correspond to the average $E^{*,\mathrm{Bf}}$ listed in the figures. Figure from Ref. [1].

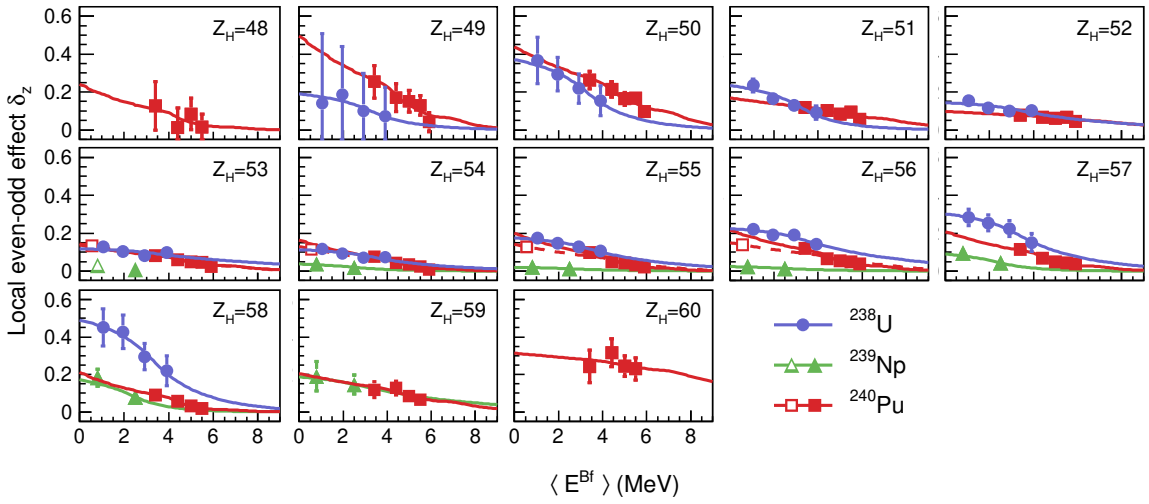

Figure 3. Evolution of δ_Z as a function of the average $E^{*,\mathrm{Bf}}$ for each split in ^{238}U (blue dots), ^{239}Np (green triangles), and ^{240}Pu (red squares). In the case of ^{239}Np, $-\delta_Z$ is plotted. Solid symbols are measured data and lines are fits to Eq. 1 folded with the experimental resolution. Empty symbols are data from [24, 25]. Red dashed lines show fits when data from [25] are included. Figure from Ref. [1].

Experimentally, the dissipation energy can be estimated by extrapolating the behaviour of δ_Z towards the barrier: $E^{*,\mathrm{dis}} = G\ln(|\delta_Z|)|_{E^{*,\mathrm{Bf}}\to\Delta}$. The parameter $G(Z)$ can be seen as the "sensitivity" of δ_Z with respect to changes in $E^{*,\mathrm{int}}$.

Figure 3 shows the evolution of δ_Z as a function of $E^{*,\mathrm{Bf}}$ for each fragment Z, fitted to Eq. 1, while Figure 4 shows the resulting $E^{*,\mathrm{dis}}$ as a function of the fragment Z. Similar features can be observed in the three systems:

Around Z=50, the dissipation seems to be very small. This is consistent with a reduced neutron evaporation, and a high TKE and short neck at the scission point [18]. A small dissipation also suggests a short fission time [3, 4, 6].

Around Z=52 there is a clear maximum, which is consistent with several level crossings and dissipation through Landau-Zener excitations in the way to produce the octupole shell [26], suggesting a longer saddle-to-scission time. This is a remarkable observation when considering that Z=52 is one of the main shells in the fragment yield distributions in actinides. Interestingly enough, the fission process in these systems favours slow and dissipative paths to form octupole-deformed fragments instead of faster and almost "friction-less" paths to produce spherical ones.

There is a sudden increase for very asymmetric splits towards Z=59 that might be explained with a fission time longer than the time to transfer protons from one pre-fragment to the other. The transfer time is expected to depend on the temperature difference of the pre-fragments. For a sufficiently big asymmetry, this transfer time is short enough for the system to move all single protons from the light to the heavy pre-fragment. In these conditions, δ_Z loses its sensitivity to the dissipation process but, in turn, it signals a point where the fission time could be deduced from the transfer time [27].

3 Proton even-odd staggering in quasi-fission

The onset of quasi-fission (QF) reactions was also recently explored in VAMOS with reactions induced from a ^{238}U beam at 5.9A MeV on a ^{27}Al target [28, 29]. The same reaction was reported previously in Refs. [30, 31], in which

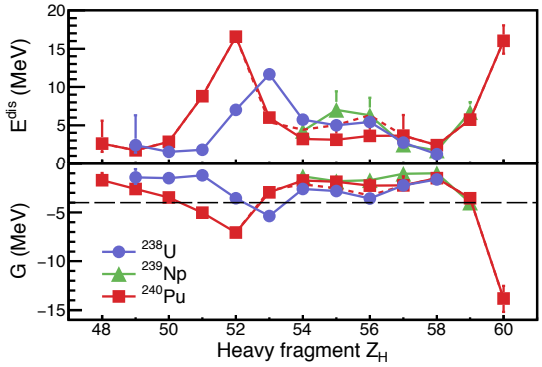

Figure 4. Deduced $E^{*,\mathrm{dis}}$ (top) and G (bottom) as a function of the heavy-fragment Z for ^{238}U (blue dots and line), ^{239}Np (green triangles and line), and ^{240}Pu (red squares and line). Red dashed lines show the results of ^{240}Pu when including data from [25]. Figure from Ref. [1].

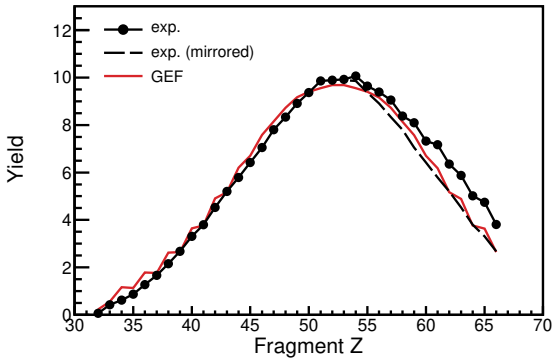

Figure 5. The figure shows the elemental yields from ^{238}U+^{27}Al collisions, measured between ~35° to ~62° in c.m. (black line and dots), compared to GEF [32] calculations for fusion-fission from the corresponding ^{265}Db compound system (red line). The black dashed line is a mirrored image around the symmetry (Z=52.5) of the experimental data.

the authors achieved complete mass-angular distributions, also in inverse kinematics. These data show a clear correlation between the c.m. angle and the fragment mass, which was interpreted as an indication of the production of QF reactions along with complete fusion-induced fission (FF). The data measured in VAMOS improves on the previous one but only in some aspects: On the one hand, the new data include the element identification of the fragments, as well as the masses and velocities in c.m. On the other hand, the angular acceptance in c.m. covers only from ~35° to ~62°.

Figure 5 shows the fragment Z distribution for fission and QF induced in ^{238}U+^{27}Al collisions. The figure also shows the prediction from GEF [32] for a ^{265}Dd fissioning system with the same conditions expected in the experimental one: an initial energy of E^*_{FS}=61.2 MeV and an angular momentum of L_{RMS}=27$\hbar$. The comparison of the experimental data with the FF results from GEF shows a clear excess of yield for heavy fragments. This is also evident when comparing heavy-fragment yields with their light counterparts, as the figure demonstrates with a mirrored image of the measured data around symmetric splits.

This yield excess is a direct consequence of measuring QF and FF events in the same data set. In QF, a strong correlation between the fragments emission angle and their mass is observed (see Ref. [33] for an extensive review on this and other properties of QF). Therefore, the event-by-event counterparts of the heavy fragments produced in QF reactions measured between ~35° and ~62° in c.m. are emitted between ~145° to ~118°, which is outside the VAMOS acceptance and thus they are not measured. Since the Z distribution from fission fragments is insensitive to the emission angle, the heavy-fragment side of the distribution is a mirrored image of the light-fragment one.

This different character of FF and QF can be used to estimate the QF yield contained in the data. The measured yield for any element Z is the sum of FF and QF yields: $Y_{\mathrm{exp}}(Z) = Y_{\mathrm{FF}}(Z) + Y_{\mathrm{QF}}(Z)$. In FF reactions, the yields of complementary fragments are equal: $Y_{\mathrm{FF}}(Z) = Y_{\mathrm{FF}}(Z_{\mathrm{FS}} - Z)$, with Z_{FS}=105 as the atomic number of the fissioning system. Therefore, after subtracting the measured light-fragment yields from the complementary heavy-fragment ones, only QF yields survive:

$$Y_{\mathrm{exp}}(Z) - Y_{\mathrm{exp}}(Z_{\mathrm{FS}} - Z) = Y_{\mathrm{QF}}(Z) - Y_{\mathrm{QF}}(Z_{\mathrm{FS}} - Z) \quad (2)$$

Assuming that the QF yield distribution in this window of c.m. angle can be approximated by a Gaussian function Gf_{QF}, the difference between yields of Eq. 2 can be fitted to obtain the underlying Gf_{QF}:

$$Y_{\mathrm{exp}}(Z) - Y_{\mathrm{exp}}(Z_{\mathrm{FS}} - Z) = Gf_{\mathrm{QF}}(Z) - Gf_{\mathrm{QF}}(105 - Z) \quad (3)$$

Figure 6 shows the difference $Y_{\mathrm{exp}}(Z) - Y_{\mathrm{exp}}(105 - Z)$ and the resulting fit to Gf_{QF}. The main position of the QF component is Z~63.5, with a width of ~5.3. The amount of QF can be also estimated from the fit, resulting in ~15% of the total FF+QF events.

Despite the relatively large error bars, a clear even-odd staggering is observed. In order to estimate its am-

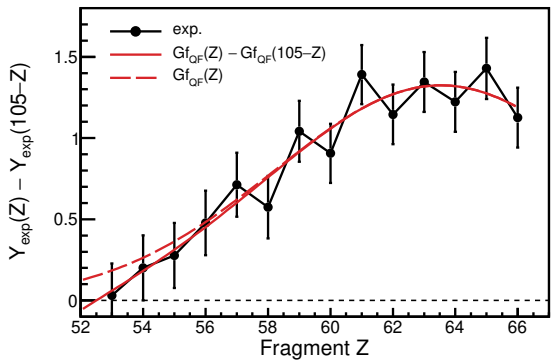

Figure 6. Difference between complementary experimental yields $Y_{\mathrm{exp}}(Z) - Y_{\mathrm{exp}}(Z_{\mathrm{FS}} - Z)$ (black line and dots). The red dashed line shows the Gf_{QF} function associated with the QF yields, while the red solid line is the difference between the Gf_{QF} function evaluated at complementary fragments, which is fitted to the experimental data (see text).

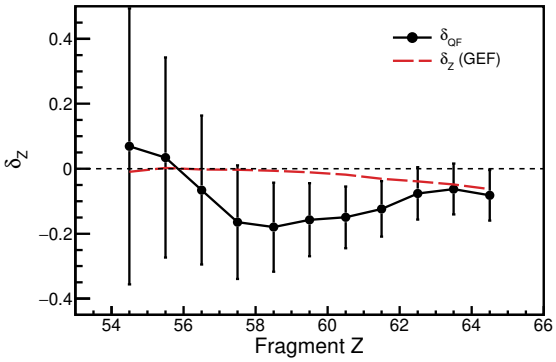

Figure 7. Local even-odd effect δ_{QF} deduced for the QF distribution obtained in Fig. 6 (black line and dots). The dashed red line shows the local even-odd effect δ_Z calculated with GEF for ^{265}Db at E^*_{FS}=7 MeV. Error bars show statistical uncertainty.

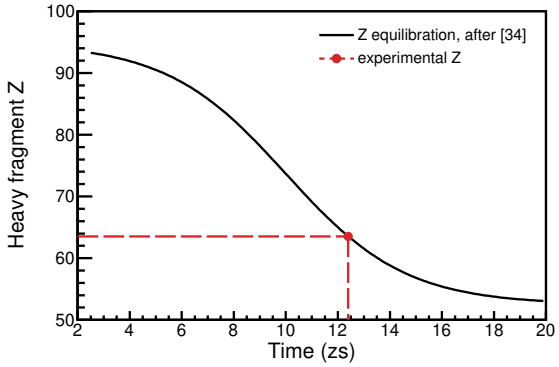

Figure 8. Evolution of heavy-fragment Z according to the mass and isospin equilibration described in [34] (black line). The red dot shows the time where the equilibration reaches the average heavy-fragment Z obtained in the experimental data, which signals the scission point for the QF reactions.

plitude, the prescription of Ref. [11] is again applied. The resulting local even-odd effect for QF, δ_{QF}, is displayed in Fig. 7. Concerning the uncertainties, these are obtained from classical error propagation of statistical uncertainties in the formula of Ref. [11]. The results show an average $\delta_{QF}\sim-0.1$, and reaching even below in the region with higher yield and statistical significance, where the probability of $\delta_{QF}\geq 0$ is less than 7%, according to the uncertainty.

$\delta_{QF}\sim-0.1$ is a remarkable value for an odd-Z system. As a means of comparison, the same figure shows the GEF calculation for a ^{265}Db fissioning system at E^*_{FS}=7 MeV. Such initial energy is close to the barrier and thus would maximise δ_Z but, even in these conditions, δ_{QF} is significantly larger than the one expected for FF reactions.

3.1 Toy model for proton even-odd staggering in quasi-fission

In order to interpret the large amplitude of δ_{QF}, we propose a simplified model to describe the movement of single protons and proton pairs within the quasi-compound system. The dynamics of the model are largely based on Ref. [34], where the time evolution of the mass and isospin asymmetry of the pre-fragments is calculated.

According to Ref. [34], QF pre-fragments attain isospin equilibration in a very short time after they get in contact and the transfer of nucleons begins. In the case of ^{238}U+^{27}Al, this implies a quick transfer of a neutron pair from ^{238}U to ^{27}Al and of the unpaired proton from ^{27}Al to ^{238}U, who, in less than 2 zs, becomes ^{237}Np. From then on, the mass drift towards equilibration dominates.

The toy model begins at the point of isospin equilibration, and proceeds in steps. Each step implies the transfer of a proton or a proton pair from the heavy pre-fragment to the light one.[1] As initial assumption, proton pairs and single protons are considered on an equal footing and having the same probability of being transferred. Although this might not be the case: as Ref. [34] points out *"the least bound nucleons (close to the Fermi surface) are usually more freely transferred"*.[2] This would imply a larger probability for single protons than for proton pairs. In this regard, this toy model works as an upper limit for the expected even-odd effect and dissipation.

If the initial ^{237}Np has no broken proton pairs, in the first step, the model has one single proton $N_{sp} = 1$ and $N_{pp} = (93 - N_{sp})/2 = 46$ proton pairs to chose from. In the case of one broken pair, $N_{sp} = 3$ and $N_{pp} = 45$, etc. The probability of transferring a single proton is $P_{sp} = N_{sp}/(N_{pp} + N_{sp})$, while that of a pair is the complementary probability $P_{pp} = 1 - P_{sp}$.

The model performs a chain of steps until reaching the mass equilibration. In each step, an entity (a single proton or a pair) is randomly selected according to their probabilities. In order to obtain the amplitude of δ_{QF}, the model simulates a large number of chains, and computes the relative difference between even- and odd-Z heavy pre-fragments, as well as the average Z, for each step.

In this form, the toy model lacks any dynamics; the steps work simply as an ordering parameter and their actual duration in time is not computed. Here is where we refer to the model of Ref. [34]: each step is associated with the time needed to reach its average Z, following the evolution of the isospin and mass equilibration. Figure 8 shows the Z equilibration after the model of Ref. [34]. The time to reach the measured average Z=63.5, and thus splitting the system, is ~12.4 zs.

Figure 9 shows the time evolution of δ_{QF} computed with this toy model assuming N_{sp}=1, 3, and 5 initial single protons, which can be directly related with initial intrinsic excitation energy in the heavy pre-fragment. A completely paired system would reach the measured Z with $\delta_{QF}\sim0.35$; however, a system with some initial energy spent in breaking proton pairs would arrive with $\delta_{QF}\sim0$. In order to reach the measured $\delta_{QF}\sim0.1$, the system would need to break between one and two pairs midway. Figure 9 shows some

[1] Although the transfer back from the light to the heavy pre-fragment might be possible, the probability is comparably very small, as FF data and models suggest; thus is not considered here for simplicity.

[2] A further dependence on the pre-fragment relative sizes and level densities may be at play although is not included.

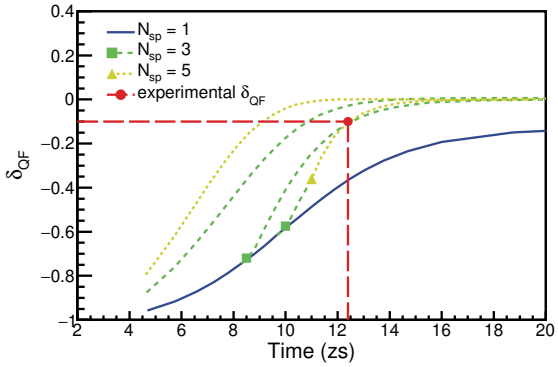

Figure 9. Evolution of δ_{QF} as a function of time computed by the present toy model. The lines show the evolution N_{sp}=1, 3, and 5 (solid blue, dashed green, and short-dashed yellow lines, respectively). Green squares show the moment where a pair is broken and N_{sp}=1 increases to N_{sp}=3, whereas the yellow triangle signals the breaking of another pair and the transition from N_{sp}=3 to N_{sp}=5. The long-dashed red lines and circle show the moment where the system reaches the average δ_{QF} measured and the QF scission point.

possible combinations: a completely paired system breaks one proton pair at ~8 zs, or, if the pair is broken slightly later, further pairs need to be broken before the scission point at 12.4 zs.[3]

This simple model shows that, even in QF reactions with long sticking times as the present one, very few pairs are broken. Therefore, the energy dissipated in single particle excitations must be of the order of the pairing gap Δ. In addition, Δ would correspond to that of the system at the moment the pair is broken. According to Fig. 9, this is around Z~75, and therefore $\Delta\approx$0.8 MeV [13]. This energy is much lower than the one expected in low-excitation fission reactions, in which the amplitude of δ_Z is maximum. A possible reason is that quasi-compound systems in QF reactions do not need to overcome a fission barrier and thus they experience a smaller drop in potential energy. Since the dissipation energy and the pair breaking are fed from this drop, it seems reasonable to expect a smaller amount of both in QF reactions.

Ref. [34] also demonstrates that the energy dissipated from the slowing down of the two nuclei once they are in contact is used in the exchange of nucleons while they reach the isospin equilibration. The present data suggests that these equilibration and dissipation stages involve the exchange of completely paired nucleons.

In addition, the fact that only few pairs are broken after the dissipation of the initial kinetic energy suggests that the fragments maintain small deformations, with few level crossings that would increase the number of broken pairs and the dissipation in the latter stage of the QF process.

Despite the reduced angular coverage, this work shows that the measurement of δ_{QF} can reveal details of the dissipation as a function of time in QF reactions. Further experiments with larger angular coverage would be able to track the amount of energy dissipated in pair breaking along the path of the quasi-compound system in the potential landscape. These experimental data could help to include pairing correlations, as well as dynamical descriptions, in models aiming for a complete understanding of QF reactions.

[3] Again, since the toy model treats single protons and proton pairs with the same probability of being transferred, the number of broken pairs is likely to be smaller.

4 Summary

The study of the even-odd staggering in isotopic yields of fission and quasi-fission fragments is a promising tool to obtain information about the dynamics of the fission and quasi-fission processes and its relation with energy dissipation, nuclear structure, and time.

Concerning fission, the systematic measurement of δ_Z as a function of the initial energy, summarised here and detailed in [1], shows a clear correlation between the energy dissipated along the process and nuclear shells in the fragments, suggesting a dependence of the fission time on the fragment split.

In the case of quasi-fission reactions, preliminary data shows a δ_Z amplitude larger than that of fission in similar conditions. Such amplitude can be explained with a very low dissipation in the quasi-compound system, largely generated with the exchange of nucleon pairs. The comparison between both reactions suggest that in fission most of the dissipation and the breaking of nucleon pairs is produced close to the barrier.

References

[1] D. Ramos et al., Phys. Rev. C **107**, L021601 (2023). https://doi.org/10.1103/PhysRevC.107.L021601
[2] M. Bender et al., J. Phys. G: Nucl. Part. Phys. **47**, 113002 (2020). https://doi.org/10.1088/1361-6471/abab4f
[3] K. T. R. Davies, A. J. Sierk, and J. R. Nix, Phys. Rev. C **13**, 2385 (1976). https://doi.org/10.1103/PhysRevC.13.2385
[4] T. Ledergerbert, Z. Paltiel, Z. Fraenkel, and H. C. Pauli, Nucl. Phys. A **275**, 280 (1977). https://doi.org/10.1016/0375-9474(77)90453-5
[5] K.-H. Schmidt and B. Jurado, Rep. Prog. Phys. **81**, 106301 (2018). https://doi.org/10.1088/1361-6633/aacfa7
[6] A. Bulgac, S. Jin, K. J. Roche, N. Schunck, and I. Stetcu, Phys. Rev. C **100**, 034615 (2019). https://doi.org/10.1103/PhysRevC.100.034615
[7] N. Schunck and D. Regnier, Prog. Part. Nucl. Phys. **125**, 103963 (2022). https://doi.org/10.1016/j.ppnp.2022.103963
[8] S. Amiel and H. Feldstein, Phys. Rev. C **11**, 845 (1975). https://doi.org/10.1103/PhysRevC.11.845
[9] S. Pommé, E. Jacobs, K. Persyn, D. De Frenne, K. Govaert, and M. L. Yoneama, Nucl. Phys. A **560**, 689 (1993). https://doi.org/10.1016/0375-9474(93)90041-U

[10] K. Persyn, E. Jacobs, S. Pommé, D. De Frenne, K. Govaert, and M. L. Yoneama, Nucl. Phys. A **620**, 171 (1997). https://doi.org/10.1016/S0375-9474(97)00156-5
[11] B. L. Tracy, J. Chaumont, R. Klapisch, J. M. Nitschke, A. M. Poskanzer, E. Roeckl, and C. Thibault, Phys. Rev. C **5**, 222 (1972). https://doi.org/10.1103/PhysRevC.5.222
[12] S. Steinhäuser et al., Nucl. Phys. A **634**, 89 (1998). https://doi.org/10.1016/S0375-9474(98)00148-1
[13] F. Rejmund, A. V. Ignatyuk, A. R. Junghans, and K.-H. Schmidt, Nucl. Phys. A **678**, 215 (2000). https://doi.org/10.1016/S0375-9474(00)00322-5
[14] M. Caamaño, F. Rejmund, and K.-H. Schmidt, J. Phys. G: Nucl. Part. Phys. **38**, 035101 (2011). https://doi.org/10.1088/0954-3899/38/3/035101
[15] M. Caamaño et al., Phys. Rev. C **88**, 024605 (2013). https://doi.org/10.1103/PhysRevC.88.024605
[16] C. Rodríguez-Tajes et al., Phys. Rev. C **89**, 024614 (2014). https://doi.org/10.1103/PhysRevC.89.024614
[17] M. Caamaño et al., Phys. Rev. C **92**, 034606 (2015). https://doi.org/10.1103/PhysRevC.92.034606
[18] M. Caamaño and F. Farget, Phys. Lett. B **770**, 72 (2017). https://doi.org/10.1016/j.physletb.2017.04.041
[19] D. Ramos et al., Phys. Rev. C **97**, 054612 (2018). https://doi.org/10.1103/PhysRevC.97.054612
[20] D. Ramos et al., Phys. Rev. C **99**, 024615 (2019). https://doi.org/10.1103/PhysRevC.99.024615
[21] D. Ramos et al., Phys. Rev. Lett. **123**, 092503 (2019). https://doi.org/10.1103/PhysRevLett.123.092503
[22] D. Ramos et al., Phys. Rev. C **101**, 034609 (2020). https://doi.org/10.1103/PhysRevC.101.034609
[23] C. Schmitt et al., Phys. Rev. Lett. **126**, 132502 (2021).https://doi.org/10.1103/PhysRevLett.126.132502
[24] I. Tsekhanovich, H.-O. Denschlag, M. Davi, Z. Büyükmumcu, F. Gönnenwein, S. Oberstedt, and H. R. Faust, Nucl. Phys. A **688**, 633 (2001). https://doi.org/10.1016/S0375-9474(00)00586-8
[25] C. Schmitt et al., Nucl. Phys. A **430**, 21 (1984). https://doi.org/10.1016/0375-9474(84)90191-X
[26] G. Scamps and C. Simenel, Nature (London) **564**, 382 (2018). https://doi.org/10.1038/s41586-018-0780-0
[27] K.-H. Schmidt and B. Jurado, Phys. Procedia **47**, 88 (2013).https://doi.org/10.1016/j.phpro.2013.06.014
[28] G. Mantovani et al., EPJ Web of Conferences **223**, 01037 (2019). https://doi.org/10.1051/epjconf/201922301037
[29] D. Fernández et al., EPJ Web of Conferences **284**, 04009 (2023). https://doi.org/10.1051/epjconf/202328404009
[30] J. Tōke et al., Phys. Lett. B **142**, 258 (1984). https://doi.org/10.1016/0370-2693(84)91194-8
[31] J. Tōke et al., Nucl. Phys. A **440**, 327 (1985). https://doi.org/10.1016/0375-9474(85)90344-6
[32] K.-H. Schmidt, B. Jurado, C. Amouroux, and C. Schmitt, Nucl. Data Sheets 131, 107 (2016). https://doi.org/10.1016/j.nds.2015.12.009.
GEF code v. 2023/1.1
[33] D. J. Hinde, M. Dasgupta, and E. C. Simpson, Prog. Part. Nucl. Phys. **118**, 103856 (2021). https://doi.org/10.1016/j.ppnp.2021.103856
[34] C. Simenel, K. Godbey, and A. S. Umar, Phys. Rev. Lett. **124**, 212504 (2020). https://doi.org/10.1103/PhysRevLett.124.212504